

## TURBULENT CORONAL HEATING AND THE DISTRIBUTION OF NANOFLARES

PABLO DMITRUK<sup>1</sup> AND DANIEL O. GÓMEZ<sup>2,3</sup>

Departamento de Física, Facultad de Ciencias Exactas y Naturales, Universidad de Buenos Aires, Ciudad Universitaria, Pabellón I,  
 1428 Buenos Aires, Argentina

Received 1997 February 12; accepted 1997 April 14

### ABSTRACT

We perform direct numerical simulations of an externally driven two-dimensional magnetohydrodynamic system over extended periods of time to simulate the dynamics of a transverse section of a solar coronal loop. A stationary and large-scale magnetic forcing was imposed, to model the photospheric motions at the magnetic loop footpoints. A turbulent stationary regime is reached, which corresponds to energy dissipation rates consistent with the heating requirements of coronal loops.

The temporal behavior of quantities such as the energy dissipation rate shows clear indications of intermittency, which are exclusively due to the strong nonlinearity of the system. We tentatively associate these impulsive events of magnetic energy dissipation (from  $5 \times 10^{24}$  to  $10^{26}$  ergs) to the so-called nanoflares. A statistical analysis of these events yields a power-law distribution as a function of their energies with a negative slope of 1.5, which is consistent with those obtained for flare energy distributions reported from X-ray observations.

*Subject headings:* MHD — Sun: flares — turbulence

### 1. INTRODUCTION

Coronal loops in active regions are likely to be heated by Joule dissipation of highly structured electric currents. The formation of small scales in the spatial distribution of electric currents is necessary to enhance magnetic energy dissipation and therefore provide sufficient heating to the plasma confined in these loops. Various scenarios of how these fine-scale structures might be generated have been proposed, such as the spontaneous formation of tangential discontinuities (Parker 1972, 1983), the development of an energy cascade driven by random footpoint motions on a force-free configuration (van Ballegoijen 1986), or the direct energy cascade associated to a fully turbulent magnetohydrodynamic (MHD) regime (Heyvaerts & Priest 1992; Gómez & Ferro Fontán 1992). These rather different models share in common the dominant role of nonlinearities in generating fine spatial structure.

In this paper we assume that the dynamics of a coronal loop driven by footpoint motions is described by the MHD equations. Since the kinetic ( $R$ ) and magnetic ( $S$ ) Reynolds numbers in coronal active regions are extremely large ( $R \sim S \sim 10^{10}$ – $10^{12}$ ), we expect footpoint motions to drive the loop into a strongly turbulent MHD regime.

Footpoint motions whose length scales are much smaller than the loop length cause the coronal plasma to move in planes perpendicular to the axial magnetic field, generating a small transverse magnetic field component. In § 2 we model this coupling to simulate the driving action of footpoint motions on a generic transverse section of the loop. The numerical technique used for the integration of the two-dimensional MHD equations is described in § 3. In § 4 we report the energy dissipation rate that we obtain, and a statistical analysis of dissipation events is presented in § 5. Finally, the relevant results of this paper are summarized in § 6.

### 2. FORCED TWO-DIMENSIONAL MAGNETOHYDRODYNAMICS

The dynamics of a coronal loop with a uniform magnetic field  $\mathbf{B} = B_0 \hat{z}$ , length  $L$ , and transverse section  $(2\pi l) \times (2\pi l)$  can be modeled by the reduced magnetohydrodynamic (RMHD) equations (Strauss 1976):

$$\partial_t a = v_A \partial_z \psi + [\psi, a] + \eta \nabla^2 a, \quad (1)$$

$$\partial_t w = v_A \partial_z j + [\psi, w] - [a, j] + \nu \nabla^2 w, \quad (2)$$

where  $v_A = B_0 / (4\pi\rho)^{1/2}$  is the Alfvén speed,  $\nu$  is the kinematic viscosity,  $\eta$  is the plasma resistivity,  $\psi$  is the stream function,  $a$  is the vector potential,  $w = -\nabla^2 \psi$  is the fluid vorticity,  $j = -\nabla^2 a$  is the electric current density, and  $[u, v] = \mathbf{z} \cdot \nabla u \times \nabla v$ . For given photospheric motions applied at the footpoints (plates  $z = 0$  and  $z = L$ ), horizontal velocity and magnetic field components develop in the interior of the loop, given by  $\mathbf{v} = \nabla \times (\mathbf{z}\psi)$  and  $\mathbf{b} = \nabla \times (\mathbf{z}a)$ .

The RMHD equations can be regarded as describing a set of two-dimensional MHD systems stacked along the loop axis and interacting among themselves through the  $v_A \partial_z$  terms. For simplicity, hereafter we study the evolution of a generic two-dimensional slice of a loop, to which end we model the  $v_A \partial_z$  terms as external forces (see Einaudi et al. 1996 for a similar approach). We assume the vector potential to be independent of  $z$  and the stream function to interpolate linearly between  $\psi(z = 0) = 0$  and  $\psi(z = L) = \Psi$ , where  $\Psi(x, y, t)$  is the stream function for the photospheric velocity field. These assumptions yield  $v_A \partial_z \psi = v_A \Psi / L$  (in eq. [1]) and  $v_A \partial_z j = 0$  (in eq. [2]) and correspond to an idealized scenario where the magnetic stress distributes uniformly throughout the loop. The two-dimensional equations for a generic transverse slice of a loop become

$$\partial_t a = [\psi, a] + \eta \nabla^2 a + f, \quad (3)$$

$$\partial_t w = [\psi, w] - [a, j] + \nu \nabla^2 w, \quad (4)$$

where  $f = (v_A / L) \Psi$ .

<sup>1</sup> Fellow of Universidad de Buenos Aires; dmitruk@df.uba.ar.

<sup>2</sup> Also at the Instituto de Astronomía y Física del Espacio, Buenos Aires, Argentina.

<sup>3</sup> Member of the Carrera del Investigador, CONICET, Argentina.

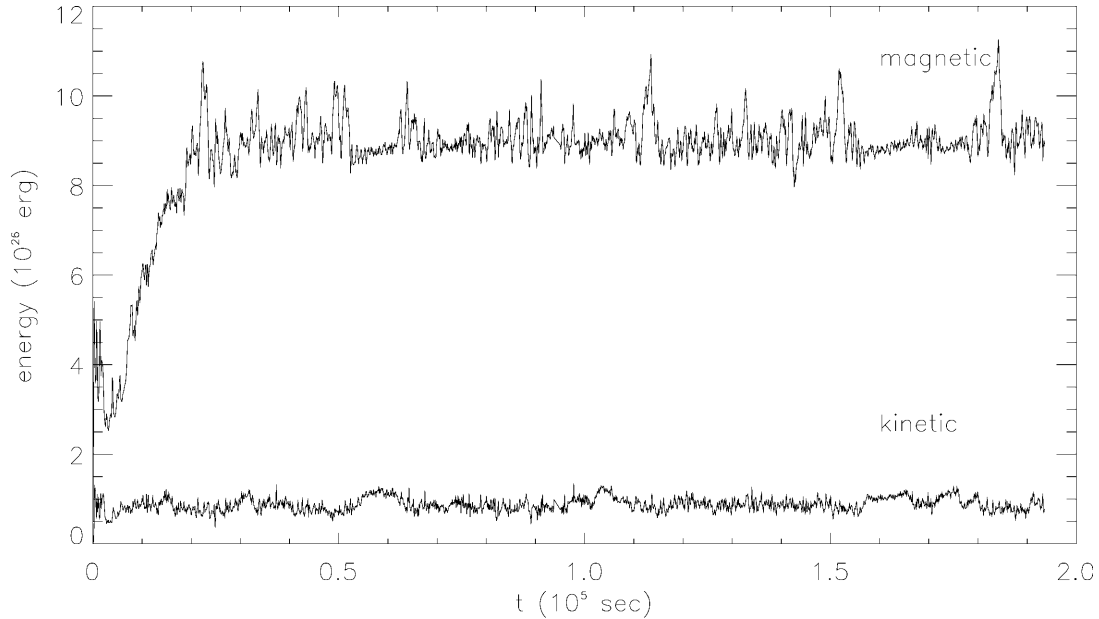


FIG. 1.—Magnetic and kinetic energy as functions of time for our simulation

### 3. NUMERICAL PROCEDURES

We performed numerical simulations of equations (3) and (4) on a square box of sides  $2\pi$ , with periodic boundary conditions. The magnetic vector potential and the stream function are expanded in Fourier series. To be able to perform long-time integrations, we worked with a moderate resolution version of the code ( $96 \times 96$  grid points). The code is of the pseudospectral type, with  $2/3$  de-aliasing (Canuto et al. 1988). The temporal integration scheme is a fifth-order predictor-corrector, to achieve almost exact energy balance over our extended time simulations.

We turn equations (3) and (4) into a dimensionless version, choosing  $l$  and  $L$  as the units for transverse and longitudinal distances and  $v_0 = (f_0)^{1/2}$  as the unit for velocities [ $f_0 = v_A u_\phi(l/L)$ ,  $u_\phi$ : typical photospheric velocity], since the field intensities are determined by the forcing strength. The dimensionless dissipation coefficients are  $\nu_0 = \nu/[l(f_0)^{1/2}]$  and  $\eta_0 = \eta/[l(f_0)^{1/2}]$ . The forcing is constant in time and nonzero only in a narrow band in  $k$  space corresponding to  $3 \leq kl \leq 4$ . In spite of the narrow forcing and even though velocity and magnetic fields are initially zero, nonlinear terms quickly populate all the modes across the spectrum, and a stationary turbulent state is reached.

### 4. ENERGY DISSIPATION RATE

To restore the dimensions to our numerical results, we used typical values for the solar corona:  $L \sim 5 \times 10^9$  cm,  $l \sim 10^8$  cm,  $v_\phi \sim 10^5$  cm s $^{-1}$ ,  $B_0 \sim 100$  G,  $n \sim 5 \times 10^9$  cm $^{-3}$ , and  $\nu_0 = \eta_0 = 3 \times 10^{-2}$ .

Figure 1 shows magnetic and kinetic energy versus time. The behavior of both energies is highly intermittent despite the fact that the forcing is constant and coherent. This kind of behavior is usually called internal intermittency, to emphasize the fact that the rapid fluctuations are not induced by an external random forcing. Also, note that magnetic energy is about 1 order of magnitude larger than kinetic energy. The energy dissipation rate is also a strongly intermittent quantity, as shown in Figure 2. For turbulent systems at large Reynolds

numbers, the dissipation rate in the stationary regime is expected to be independent of the Reynolds number  $R$  (Kolmogorov 1941). For the rather moderate Reynolds number simulations reported here, a weak (monotonically increasing) dependence of the dissipation rate with  $R$  still remains (see also Einaudi et al. 1996). The total dissipation rate for the typical numbers listed above is  $\epsilon \approx 1.6 \times 10^{24}$  ergs s $^{-1}$ . We can transform the heating rate into an energy influx from the photosphere, by simply dividing by twice the transverse area (because we have two boundaries), i.e.,  $\mathcal{F} = \epsilon/[2(2\pi l)^2]$ . In equation (5) we show the quantitative value of the energy flux as well as the explicit dependence with the relevant parameters of the problem:

$$\mathcal{F} = 2 \times 10^6 \frac{\text{ergs}}{\text{cm}^2 \text{ s}} \left( \frac{n}{5 \times 10^9 \text{ cm}^{-3}} \right)^{1/4} \times \left( \frac{B_0}{100 \text{ G}} \right)^{3/2} \left( \frac{u_{\text{ph}}}{10^5 \text{ cm s}^{-1}} \right)^{3/2} \frac{(l_{\text{ph}}/10^8 \text{ cm})^{1/2}}{(L/5 \times 10^9 \text{ cm})^{1/2}}. \quad (5)$$

This energy flux compares quite favorably with the heating requirements for active regions, which span the range  $\mathcal{F} = 3 \times 10^5$ – $10^7$  ergs cm $^{-2}$  s $^{-1}$  (Withbroe & Noyes 1977).

### 5. DISTRIBUTION OF NANOFLARES

In this section, we associate the peaks of energy dissipation displayed in Figure 2 with the so-called nanoflares (Parker 1988). We estimate the occurrence rate for these nanoevents, i.e., the number of events per unit energy and time  $P(E) = dN/dE$ , so that

$$\mathcal{R} = \int_{E_{\text{min}}}^{E_{\text{max}}} dE P(E) \quad (6)$$

is the total number of events per unit time and

$$\epsilon = \int_{E_{\text{min}}}^{E_{\text{max}}} dE E P(E) \quad (7)$$

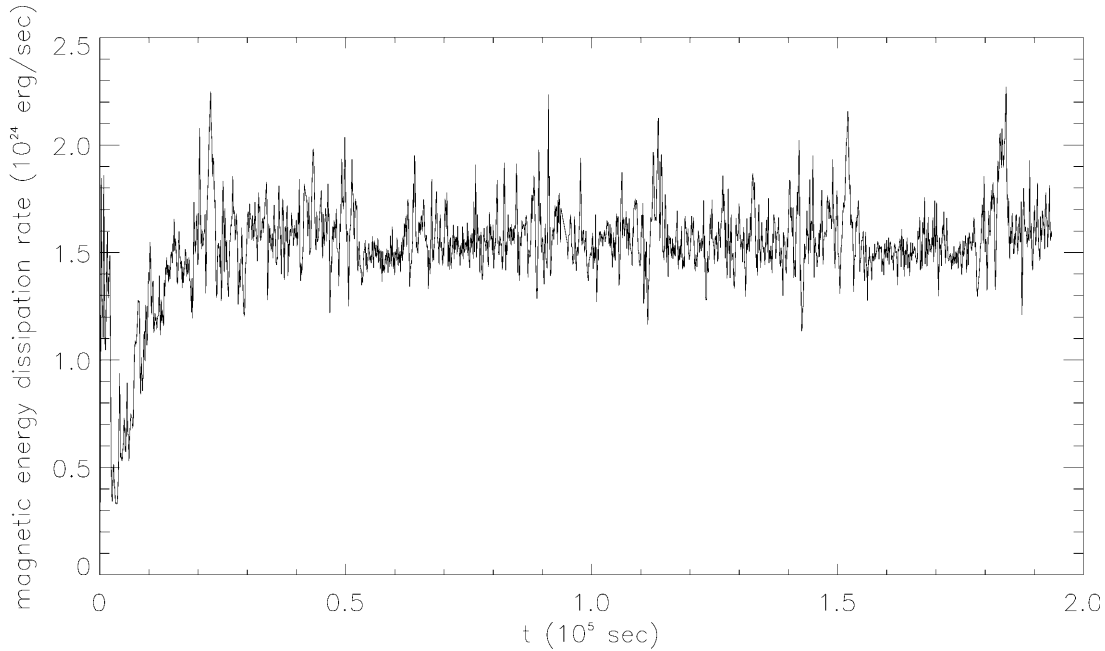


FIG. 2.—Magnetic energy dissipation rate as a function of time

is the total heating rate (in  $\text{ergs s}^{-1}$ ) contributed by all events in the energy range  $[E_{\min}, E_{\max}]$ . A simple inspection of the  $\epsilon(t)$  time series shown in Figure 2 indicates that these events are in a highly concentrated or piled-up regime; i.e., their event rate  $\mathcal{R}$  multiplied by their typical duration is much larger than unity. At any given time, many events are going on simultaneously.

This piled-up scenario is a serious drawback against performing any kind of statistical analysis. To overcome this difficulty we define an event in the following fashion: (1) we set a threshold heating rate  $\epsilon_0$  on the time series displayed in Figure 2 of the order of its time average; (2) events are excesses of dissipation that start when  $\epsilon(t)$  surpasses  $\epsilon_0$  and finish when  $\epsilon(t)$  returns below  $\epsilon_0$ . Once a particular threshold is set, we perform a statistical analysis of the events, keeping track of their peak values, durations, and total energy content. The implicit assumption behind our working definition is that the small fraction of events that emerges over the threshold are statistically representative of the whole set. We do not make any attempt to prove this assertion, which therefore remains as a working hypothesis.

Among the interesting results of this statistical analysis, we find a significant correlation between the energy and duration of events like  $E \simeq \tau^2$  (Dmitruk & Gómez 1997), which is consistent with the correlation reported by Lee, Petrosian, & McTiernan (1993) from hard X-ray observations and by Lu et al. (1993) for an avalanche model of flare occurrences. Perhaps the most important result is that the occurrence rate as a function of energy displays a power-law behavior

$$P(E) = AE^{-1.5 \pm 0.2} \quad (8)$$

in the energy range spanned from  $E_{\min} \simeq 5 \times 10^{24} \text{ergs}$  to  $E_{\max} \simeq 10^{26} \text{ergs}$ .

We define the constant  $A$  in equation (8) so that the heating rate computed from equation (7) matches the total heating rate from our simulation (see eq. [5]). Figure 3 shows our occurrence rate, displaying the power-law behavior indicated

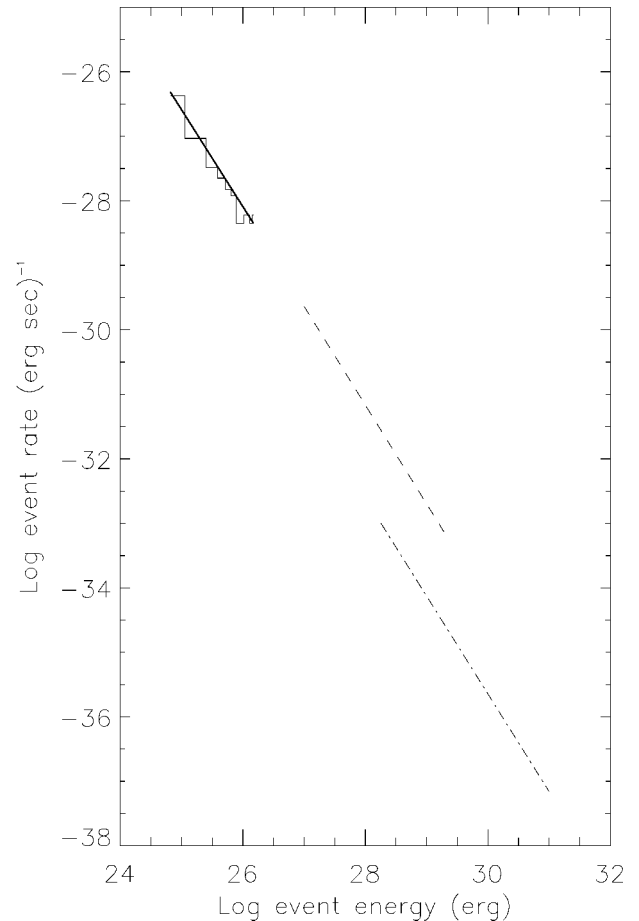


FIG. 3.—Number of events per unit energy and time. In the upper left-hand corner we plotted the histogram for our simulation; the thick line shows the best power-law fit (slope  $1.5 \pm 0.2$ ). The dashed line corresponds to the occurrence rates derived by Shimizu (1995), and the dot-dashed line corresponds to the distributions computed by Crosby et al. (1993).

in equation (8). For comparison, we also plotted the occurrence rate for transient brightenings derived by Shimizu (1995) (slope between 1.5–1.6) from *Yohkoh* soft X-ray observations and by Crosby, Aschwanden, & Dennis (1993) (slope 1.53) from *SMM* hard X-ray data. Also, we obtained the distribution of events as a function of peak fluxes that is a power law with slope  $1.7 \pm 0.3$ . This slope is consistent with the one derived by Crosby et al. (1993) (1.68) from X-ray events and somewhat flatter than those reported by Hudson (1991) (1.8). Note that the slopes derived from X-ray observations assume that the luminosity in X-rays is proportional to the dissipated energy. Porter, Fontenla, & Simnett (1995) criticize this assumption after comparing the UV and X-ray emission for several microflares and finding that slopes derived from X-rays become slightly steeper when corrected for this effect.

The remarkable correspondence between the rates plotted in Figure 3 is indicative of the presence of a common physical process behind the dissipation events ranging from  $10^{24}$  ergs or less to  $10^{33}$  ergs for the largest flares. Since in all cases the index of the power law remains smaller than 2, equation (7) implies that the contribution to energy dissipation in a given energy range ( $[E_{\min}, E_{\max}]$ ) is dominated by the most energetic events (i.e.,  $E \simeq E_{\max}$ ). According to this result, the relatively infrequent large-energy events contribute more to the heating rate than the much more numerous small energy events. This assertion might change only if indications of a turnup of the slope (to an index larger than 2) are found at low energies (Hudson 1991).

## 6. DISCUSSION AND CONCLUSIONS

In the present paper we simulate the dynamics of a transverse section of a solar coronal loop through an externally driven two-dimensional MHD code. The relevant results of this study are summarized as follows: (1) for an external forcing that is narrowband in wavenumber, we find that the system becomes strongly turbulent, and after about 20 photospheric turnover times a stationary turbulent regime is reached; (2) the energy dissipation rate obtained for typical footpoint velocities is consistent with the power necessary to heat active region loops ( $\mathcal{F} \simeq 2 \times 10^6$  ergs  $\text{cm}^{-2} \text{s}^{-1}$ ); (3) the energy dissipation rate displays a highly intermittent behavior, which is a ubiquitous characteristic of turbulent systems; (4) we associate the elementary events that compose this intermittent heating rate to the so-called nanoflare events described by Parker (1988). A statistical analysis of the events performed on a long-term numerical simulation (about 200 turnover times) shows a power-law event rate going like  $dN/dE \sim E^{-1.5}$ , which is remarkably consistent with the statistics of flare occurrence derived from observations (Hudson 1991; Crosby et al. 1993; Lee et al. 1993; Shimizu 1995).

We acknowledge financial support by the University of Buenos Aires (grant EX247) and by Fundación Antorchas.

## REFERENCES

- Canuto, C., Hussaini, M. Y., Quarteroni, A., & Zang, T. A. 1988, *Spectral Methods in Fluid Dynamics* (New York: Springer)
- Crosby, N. B., Aschwanden, M. J., & Dennis, B. R. 1992, *Sol. Phys.*, 143, 275
- Dmitruk, P., & Gómez, D. O. 1997, in preparation
- Einaudi, G., Velli, M., Politano, H., & Pouquet, A. 1996, *ApJ*, 457, L113
- Gómez, D. O., & Ferro Fontán, C. 1992, *ApJ*, 394, 662
- Heyvaerts, J., & Priest, E. R. 1992, *ApJ*, 390, 297
- Hudson, H. S. 1991, *Sol. Phys.*, 133, 357
- Kolmogorov, A. N. 1941, *Dokl. Acad. Nauk. SSSR*, 30, 301
- Lee, T. T., Petrosian, V., & McTiernan, J. M. 1993, *ApJ*, 412, 401
- Lu, E. T., Hamilton, R. J., McTiernan, J. M., & Bromund, K. R. 1993, *ApJ*, 412, 841
- Parker, E. N. 1972, *ApJ*, 174, 499
- . 1983, *ApJ*, 264, 642
- . 1988, *ApJ*, 330, 474
- Porter, J. G., Fontenla, J. M., & Simnett, G. M. 1995, *ApJ*, 438, 472
- Shimizu, T. 1995, *PASJ*, 47, 251
- Strauss, H. 1976, *Phys. Fluids*, 19, 134
- van Ballegooijen, A. A. 1986, *ApJ*, 311, 1001
- Withbroe, G. L., & Noyes, R. W. 1977, *ARA&A*, 15, 363